Available online at www.sciencedirect.com
SCIENCE DIRECT®
Catalysis Today 88 (2004) 169–181
CATALYSIS TODAY
www.elsevier.com/locate/cattod

Dehalogenative oligomerization of dichlorodifluoromethane catalyzed by activated carbon-supported Pt–Cu catalysts: effect of Cu to Pt atomic ratio

Debasish Chakraborty, Parag P. Kulkarni[1], Vladimir I. Kovalchuk, Julie L. d'Itri*

Department of Chemical Engineering, University of Pittsburgh, Pittsburgh, PA 15261, USA

Abstract

Activated carbon-supported Pt–Cu catalysts with a Cu to Pt atomic ratio in the range of 2–18 catalyze the formation of oligomerization hydrocarbon products from an equimolar mixture of CF_2Cl_2 and H_2 at 523 K. The steady-state selectivity toward C_{2+} products is 42% for the Pt1Cu2/C and increases to more than 70% when the Cu/Pt atomic ratio reaches 18:1. All catalysts deactivate with time on stream. The results of the TEM investigation are consistent with the suggestion that deactivation is attributed to carbon deposition and not to particle sintering. All of the catalysts have approximately the same average size of Pt-containing particles, independent of Cu/Pt atomic ratio, and the average size is essentially the same for the freshly reduced and used Pt–Cu catalysts. As the Cu to Pt atomic ratio is increased, a larger fraction of Cu is unalloyed with Pt. The performance of the catalysts in the $CF_2Cl_2 + H_2$ reaction is discussed in terms of the different active sites, which catalyze different elementary reaction steps.

Keywords: Dichlorodifluoromethane; Difluoromethane; Ethylene; Tetrafluoroethylene; Hydrodechlorination; Hydrodehalogenative oligomerization; Activated carbon; Platinum; Copper; Bimetallic catalysts

1. Introduction

Chlorofluorocarbons (CFCs) have had a lasting effect on the environment. They are a major source of stratospheric chlorine, which is responsible for the depletion of the ozone layer [1]. While many western countries have stopped the production of CFCs, over 350,000 Mt of CFCs were produced worldwide in the year of 2001 [2]. Thus, technology to convert CFCs into environmentally benign and industrially useful products is still required. Catalytic hydrodechlorination has obvious economic merits, because the resulting products can be recovered and recycled for use in addition to the environmental advantages [3].

Among CFCs, dichlorodifluoromethane has attracted a lot of attention, because a considerable amount of this CFC is still used in many applications or is stored. In addition, CCl_2F_2 is a convenient probe molecule to investigate fundamental issues of catalysis by supported metal particles. Historically, studies of CF_2Cl_2 conversion reactions have focused mainly on the removal of both Cl atoms to form CH_2F_2 [4–28], a suitable replacement for CF_2Cl_2 in heavy duty cooling applications [8,9]. The dehalogenative oligomerization of CF_2Cl_2 to form partially or completely dehalogenated C_{2+} products has not been extensively investigated and is the focus of this work.

* Corresponding author. Tel.: +1-412-624-9634.
E-mail address: jditri@pitt.edu (J.L. d'Itri).
[1] Present address: GE Energy and Environmental Research, 18 Mason, Irvine, CA 92618, USA.

0920-5861/$ – see front matter © 2003 Elsevier B.V. All rights reserved.
doi:10.1016/j.cattod.2003.11.012

Several investigations have shown that C_2 hydrocarbons formed as side products of CF_2Cl_2 hydrodechlorination catalyzed by both supported Pd [9,11] and Pd black [29]. Tetrafluoroethylene was reported to form over Pd–Fe/graphite and Pd–Co/graphite with a selectivity up to 25% [5], whereas the selectivity toward C_2 fluorocarbons ranged from 25 to 44% when mono- and bimetallic Ni particles supported on activated carbon were used as catalysts [30]. In general, CF_2Cl_2/H_2 ratios greater than unity favor oligomerization selectivity with Pd- and Ni-based catalysts.

A systematic investigation of the oligomerization selectivity of Group VIII noble metals which catalyzed the $CF_2Cl_2 + H_2$ reaction was performed by Kulkarni et al. [31]. It was shown that at a CFC/H_2 ratio of 1, Pd/C catalyzed the formation of C_2 and C_3 hydrocarbons with ∼75% selectivity with C_2H_4 being the major coupling product. Although Pt/C was the most active, it exhibited negligible selectivity toward coupling products (total selectivity <5%) [31]. However, the addition of Cu to the Pt/C dramatically increased the oligomerization selectivity [32]. The reaction product composition was the time dependent. At early time on stream (TOS) (15–25 h) the Pt–Cu/C catalyst with a Cu/Pt atomic ratio of 6 produced mainly C_2–C_4 hydrocarbons (∼50% selectivity). At the same time the selectivity toward tetrafluoroethylene increased at the expense of the C_2–C_4 hydrocarbons to ∼20% during 60 h on stream. Both the Pt and the Pt–Cu catalysts significantly deactivated with TOS [31,32].

Several mechanistic studies provided results consistent with the idea that surface carbene species are the common intermediate of the CF_2Cl_2 hydrodechlorination and dehalogenative oligomerization reactions [4,8,9,11,12,33]. As carbenes on the surface of Cu readily couple [34], it was hypothesized that the $:CF_2$ and $:CH_2$ carbenes formed on the exposed Cu atoms would couple to form C_{2+} products [32]. If the carbenes form on Pt, they would rapidly hydrogenate to form C_1 molecules. It was further proposed that H atoms formed by H_2 dissociation on Pt diffuse onto the Cu sites located around Pt and react with the adsorbed Cl and F atoms to regenerate the sites. If this hypothesis is correct, oligomerization selectivity would increase as the size of the Pt ensembles decreased. The hypothesis can be tested by correlating product selectivity to the change in the Cu to Pt atomic ratio in the Pt–Cu catalysts while maintaining the Pt loading constant. As Pt and Cu are completely miscible [35], one can expect that increasing the Cu in the catalyst will decrease the average size of Pt islands on the surface of Pt–Cu particles. To this end, a series of activated carbon-supported Pt–Cu catalysts with Cu/Pt atomic ratio varied from 2 to 18 was tested in the $CF_2Cl_2 + H_2$ reaction. In addition, the fresh and used catalysts were characterized with high resolution transmission electron microscopy (HRTEM) in the efforts to understand the nature of catalyst deactivation.

2. Experimental

2.1. Catalyst preparation and routine characterization

Activated carbon (BPL F3, 6 × 16 mesh, Calgon Carbon) was crushed and sieved. A fraction of 24–60 mesh (1400 m^2/g surface area; 2.4 nm, average pore diameter, BET data) was used as a support. It was co-impregnated with aqueous solutions of $H_2PtCl_6{\cdot}6H_2O$ (Alfa, 99.9%) and $CuCl_2{\cdot}2H_2O$ (MCB Manufacturing Chemists, 99.5%) to obtain Pt–Cu/C catalysts of different Pt to Cu ratio. In each case the material was allowed to equilibrate overnight before drying at ambient temperature and pressure for 24 h. It was then dried at 373 K for 2 h in vacuum (∼3.3 kPa). The catalyst nomenclature is based on the metal atomic ratio. For example, Pt1Cu6/C refers to a Pt/Cu atomic ratio of 1:6. The compositions of all the catalysts are listed in Table 1.

Carbon monoxide chemisorption measurements were conducted at 308 K with a volumetric sorption analyzer ASAP 2010 Chemi (Micromeritics®). The adsorbate to metal ratios (Table 1) were determined from irreversibly adsorbed CO; the adsorption stoichiometry was assumed to be 1. As metallic Cu does not adsorb CO irreversibly [36,37], the metal to adsorbate ratio provides a fraction of Pt atoms exposed. The equivalent average diameter of the metal particles, assuming a spherical geometry, was calculated according to the formula [38]:

$$d_{VA} = \frac{6V}{A}, \quad (1)$$

where A is the total surface area of the dispersed metal and V the total volume of the metal in the sample. Prior

Table 1
Composition of the Pt–Cu/C catalysts and the dispersion data

Catalyst composition	Pt/Cu atomic ratio	Pretreatment	CO/Pt_t[a] (%)	d_{VA}[b] (Å)	d_{ss}[c] (Å)
0.5 wt.% Pt	∞	Reduction with flowing H_2 at 673 K for 1 h	29	38	30
0.5 wt.% Pt	∞	Reduction with flowing H_2 at 673 K for 1 h followed by exposure to a HCl flow at 673 K for 20 h	n.d.[d]	–	∼20[e]
0.5 wt.% Pt	∞	Reduction with flowing H_2 at 673 K for 1 h followed by $CF_2Cl_2 + H_2$ reaction for 70 h	n.d.[d]	–	17
0.5 wt.% Pt + 0.3 wt.% Cu	1:2	Reduction with flowing H_2 at 673 K for 1 h	15	75	∼30[e]
0.5 wt.% Pt + 0.3 wt.% Cu	1:2	Reduction with flowing H_2 at 673 K for 1 h followed by $CF_2Cl_2 + H_2$ reaction for 70 h	n.d.[d]	–	∼25[e]
0.5 wt.% Pt + 1.0 wt.% Cu	1:6	Reduction with flowing H_2 at 673 K for 1 h	23	50	∼30[e]
0.5 wt.% Pt + 1.0 wt.% Cu	1:6	Reduction with flowing H_2 at 673 K for 1 h followed by $CF_2Cl_2 + H_2$ reaction for 70 h	n.d.[d]	–	24
0.5 wt.% Pt + 1.4 wt.% Cu	1:9	Reduction with flowing H_2 at 673 K for 1 h	27	42	∼30[e]
0.5 wt.% Pt + 1.4 wt.% Cu	1:9	Reduction with flowing H_2 at 673 K for 1 h followed by $CF_2Cl_2 + H_2$ reaction for 70 h	n.d.[d]	–	∼25[e]
0.5 wt.% Pt + 2.8 wt.% Cu	1:18	Reduction with flowing H_2 at 673 K for 1 h	22	53	∼30[e]
0.5 wt.% Pt + 2.8 wt.% Cu	1:18	Reduction with flowing H_2 at 673 K for 1 h followed by $CF_2Cl_2 + H_2$ reaction for 70 h	n.d.[d]	–	∼25[e]

[a] Apparent Pt dispersion determined from the chemisorption measurements.
[b] Equivalent spherical particle diameter calculated as $d_{VA} = 6V/A$ (A is the total surface areas of the dispersed metal, V the total volume of the metal) [38].
[c] Surface weighed average metal particle size determined from the HRTEM images.
[d] Not determined.
[e] Average metal particle diameter is estimated based on the measurement of the diameters of 20–40 particles.

to the CO chemisorption measurement, the catalyst was exposed to flowing H_2 at 573 K for 2 h and then at 673 K for 1 h. Afterwards, it was evacuated at 673 K for 1.5 h and cooled to the measurement temperature.

2.2. HRTEM characterization

HRTEM images were obtained using a JEOL JEM2010 instrument with a lattice resolution of 1.4 Å and an accelerating voltage of 200 kV. Selected area diffraction (SAD) was used for the phase identification. Computer simulated fast Fourier transform images and Fourier filtration were used for in-depth analyses of the structures of the particles. The surface weighed average particle sizes, d_{ss}, were calculated with the following formula:

$$d_{ss} = \frac{\sum_1^N d_i^3}{\sum_1^N d_i^2}. \quad (2)$$

For the detailed investigations, statistics were based on measurements of the diameters of the 300–500 particle images. However, for the majority of samples only a rough estimate of the average metal particle size was obtained from the measurements of 20–40 particles. The samples for electron microscopy were prepared in air by grinding the catalyst in an agate mortar with ethanol, followed by suspending the powder in ethanol using ultrasonic treatment ($\leq$5 W cm^{-2}). Then the resulting aerosol was deposited on thin, holey amorphous carbon films with a depth of 100–200 Å supported on the standard gold grids.

2.3. Catalytic experiments

The hydrodehalogenative oligomerization of CF_2Cl_2 (Atochem, purity >99%; detectable impurities: $CHF_2Cl \sim 0.25\%$ and $CH_3CF_3 \sim 0.25\%$) was conducted at atmospheric pressure in a stainless steel flow reaction system consisting of a down-flow quartz microreactor (10 mm i.d.) equipped with a quartz frit to support the catalyst. An electric furnace was used to heat the reactor zone containing the catalyst. The catalyst bed temperature was measured and controlled with an accuracy of ±1 K (Omega model CN2011).

The gas flows (CFC, H_2 and He) were metered with mass flow controllers (Brooks Instruments model 5850E) and mixed prior to entering the reactor. The reactor effluent was analyzed by an on-line GC and by a GC/MS to identify the reaction products. In addition, a 16-loop sampling valve (VICI) was attached to the GC to collect samples during the very early stages of the reaction. The samples stored in the sampling valve were analyzed after completion of the reaction. The GC (HP 5890 series II) was equipped with a 15 ft 60/80 Carbopack B/5% Fluorocol packed column (Supelco) and a flame ionization detector (FID) capable of detecting concentrations >1 ppm for all CFCs, chlorocarbons and hydrocarbons being studied. The on-line HP GC/MS system consisted of a HP 5890 series II Plus GC equipped with a Fluorocol column connected to a HP 5972 Mass Selective Detector.

Prior to reaction, the catalyst was treated with a mixture of H_2 (20 ml min^{-1}) and He (30 ml min^{-1}) (Praxair, each 99.999%) as it was heated from 300 to 673 K at the rate of 5 K min^{-1} and held at 673 K for 2 h. In some cases the H_2 pretreatment was followed by a treatment in a 10% HCl + N_2 (Liquid Carbonic, 99.999%) flow (30 ml min^{-1}) at 523 K for 20 h. The catalyst was then cooled in flowing He (30 ml min^{-1}) to 523 K, the reaction temperature, and the reactant mixture was introduced. The CF_2Cl_2 was dehalogenated at a CF_2Cl_2:H_2 ratio of 1 (2 ml min^{-1} of each) with He (26 ml min^{-1}) as a diluent. The CF_2Cl_2:H_2 ratio used in this work is the stoichiometric ratio required for the dechlorinative dimerization of CF_2Cl_2 to form C_2F_4. The mass transfer limitations were excluded by verifying that the rate of reaction (μmol of reactant reacted/g of catalyst/s) for the most active catalyst (Pt/C) remained constant (±10%) with total flow rates of 5–90 ml min at a constant temperature and concentration. For almost all experiments the conversion was maintained below 5 mol.% with 30 mg of the catalyst and the differential reactor model was assumed. Each experiment was stopped after 70 h on stream.

The selectivities (S_i) toward detectable carbon-containing products were calculated as follows:

$$S_i = \frac{n_i C_i}{\sum_i n_i C_i}, \quad (3)$$

where n_i and C_i the number of carbon atoms in a molecule and the mole fraction of the product i in the effluent gas. The HCl and HF were detected by GC/MS, but not quantified.

3. Results

3.1. Catalyst dispersion

The results of the chemisorption measurements of the reduced carbon-supported Pt and Pt–Cu catalysts are shown in Table 1. For the Pt/C, 29% of Pt atoms in the catalyst are exposed to CO chemisorption after reduction at 673 K with flowing H_2 for 1 h. This dispersion corresponds to the average diameter of the metal particles of 38 Å, assuming a spherical geometry. The CO/Pt ratios are in the range of 15–27% for the bimetallic Pt–Cu, which corresponds to spherical particle diameter in the range of 75–42 Å.

In addition to the CO chemisorption measurements, an electron microscopic investigation of the fresh and used Pt and Pt–Cu catalysts was conducted to determine the extent to which the supported metal particles sintered during the $CF_2Cl_2 + H_2$ reaction. The CO chemisorption measurements alone are insufficient to distinguish if the dispersion loss is caused by metal particle sintering, by blocking Pt surface atoms by carbonaceous deposits or by surface enrichment in Cu. As shown in Table 1, the average metal particle size of reduced fresh catalysts is ∼30 Å, independent of the Cu loading (Table 1). Exposure to the $CF_2Cl_2 + H_2$ reaction mixture at 523 K for 70 h decreased metal particle sizes of the catalysts (Table 1 and Fig. 1). The redispersion is most significant for the used Pt/C. The average Pt particle size decreased from 30 Å for the fresh catalyst to 17 Å for the used sample, and the particle size distribution substantially narrows (Fig. 1). Exposure of the reduced Pt/C to the HCl flow at 673 K had the same impact on the Pt dispersion as the $CF_2Cl_2 + H_2$ reaction mixture. The average metal particle size decreased from 30 to ∼20 Å during a 20 h HCl treatment of the fresh catalyst (Table 1). The effect of the reaction mixture on the metal particle sizes of the Pt–Cu catalysts was less profound, but quite distinct. The difference between the average particle size before and after the $CF_2Cl_2 + H_2$ reaction was approximately 5 Å (Table 1). The metal particle size distributions for the Pt–Cu catalysts also narrow during exposure to the $CF_2Cl_2 + H_2$ mixture (not shown).

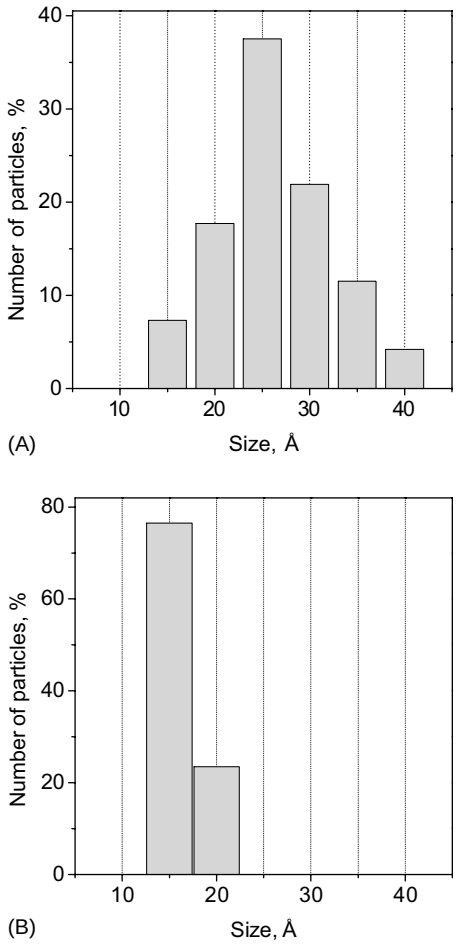

Fig. 1. Metal particle size distribution for the Pt/C catalyst after reduction with H_2 at 623 K for 1 h (A) and after exposure of the reduced catalyst to the $CF_2Cl_2 + H_2$ reaction mixture at 523 K for 70 h (B).

It is worth noting that the equivalent spherical diameter calculated from the chemisorption data and that determined from the electron microscopic investigation are in good agreement for the Pt/C. For the Pt–Cu/C, the average particle sizes calculated from the chemisorption data are 40–150% larger than those obtained from the electron microscopic images.

3.2. Catalyst microstructure

According to the SAD patterns, only particles of metallic Pt evenly distributed over the support surface are present in the reduced Pt/C catalyst (Fig. 2). The

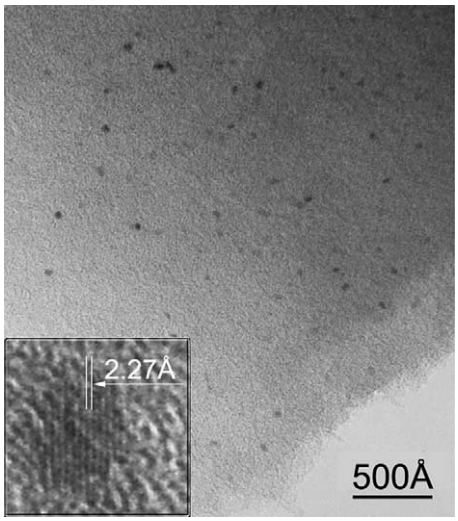

Fig. 2. TEM micrograph of the reduced Pt/C. High resolution TEM image of a Pt particle is shown in the inset.

HRTEM images of the particles exhibit fringes with interlayer distance of 2.27 Å that are also characteristic of metallic Pt. After the reduced Pt/C was exposed to a HCl flow at 673 K for 20 h there were non-metallic spherical particles approximately 200–600 Å in diameter with a much lower contrast than that of metallic Pt particles (Fig. 3). The interlayer distance of the lattice

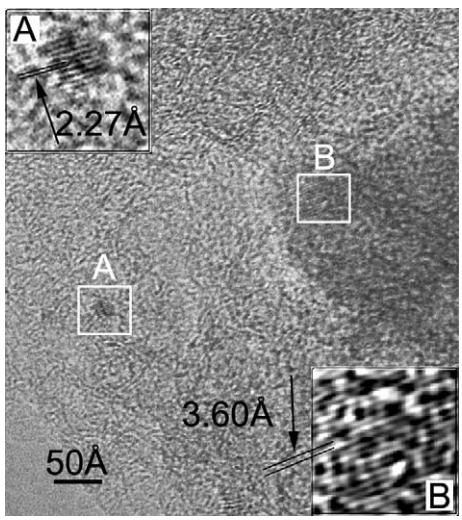

Fig. 3. TEM micrograph of the reduced Pt/C exposed to HCl at 673 K for 20 h. High resolution images of a Pt particle (A) and a non-metallic particle (B) are shown in the inset.

of these particles measured from the HRTEM images was 3.6 Å. However, it is very difficult to determine the phase composition of these particles based solely on the TEM data. Non-metallic particles with fringes corresponding to the interlayer distance of 2.5 Å were also detected in the Pt/C catalyst that was used in reaction. This distance is close to that of $PtCl_2$ [39].

A typical HRTEM micrograph of the metallic particles for the Pt–Cu catalysts is shown in Fig. 4A. Analyses of the images showed that the particles had an interlayer distance of 2.27 Å, characteristic of metallic Pt. The bimetallic catalysts also contained quasispherical particles that were empty inside (Fig. 4B). These particles were identified by their SAD patterns and by lattice interlayer distances (2.5 Å) to be CuO [40]. The presence of CuO in the catalysts is not surprising because the samples for the TEM investigation were prepared in air. The average size of the oxide particles depended on the Cu loading. For the Pt1Cu9/C, the particle size ranged from 200 to 500 Å. With the Pt1Cu18/C the particles were as large as 5000 Å and were also quasispherical. In addition, "dot" scattering centers with unusually high contrast were observed for the Pt–Cu catalysts. Typical images of such centers are shown in Fig. 5. These centers may be associated with the presence of Cu ions on the carbon surface. Ions more effectively scatter electrons than neutral atoms [41].

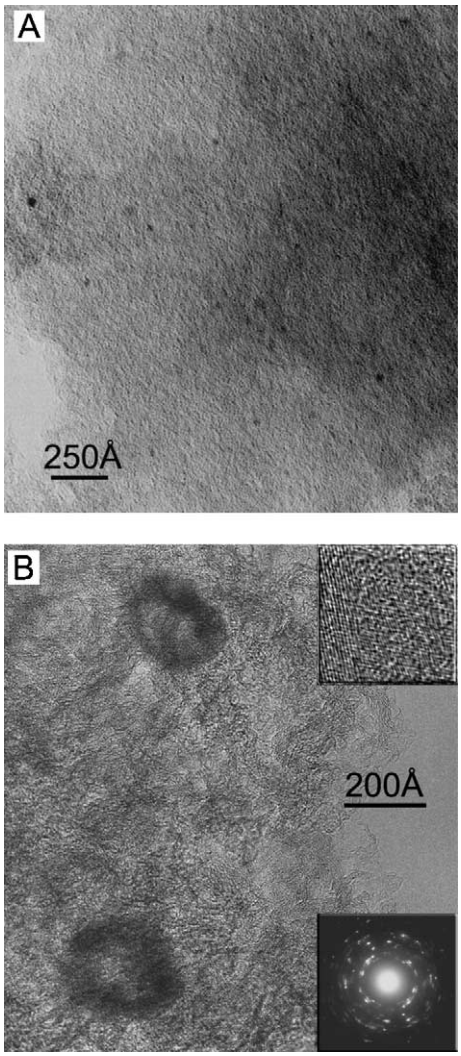

Fig. 4. TEM micrograph of the Pt1Cu9/C with metallic (A) and non-metallic particles (B). High resolution image and SAD pattern of a non-metallic particle are shown in the top and bottom insets, respectively.

3.3. Reaction kinetics

The characteristics of the CF_2Cl_2 dehalogenative oligomerization reaction catalyzed by Pt/C and Pt–Cu/C are shown in Table 2. The Pt/C and the Pt1Cu2/C exhibited the highest initial TOF of 22.4 and 23.8 s^{-1}, respectively. The rates for the other three Pt–Cu catalysts ranged between 9.3 s^{-1} for the Pt1Cu6/C and 12.3 s^{-1} for the Pt1Cu18/C. For all catalysts, the

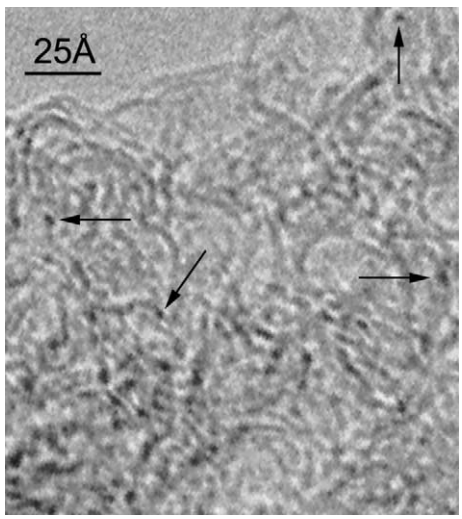

Fig. 5. "Dot" scattering centers of the reduced Pt1Cu2/C.

Table 2
Difluorodichloromethane dehalogenative oligomerization catalyzed by Pt/C and (Pt–Cu)/C

Catalyst	Initial[a] TOF[b] ($\times 10^2$ s^{-1})	Conversion (%)			Selectivity (mol%)											
		Initial[a]	Maximal	Final[c]	Initial[a]						Final[c]					
					CH_4	CH_2F_2	Other C_1[d]	C_2[e]	C_3[f]	C_{4+}[g]	CH_4	CH_2F_2	Other C_1[d]	C_2[e]	C_3[f]	C_{4+}[g]
Pt	22.4	7.0	16.0	2.0	15	53	30	1	Trace[h]	0	65[i], 40	15[j], 33	15[i], 22	4[i], 4	1[i], 1	0[i], trace[h]
Pt[j]	n.d.[k]	3	n.d.[k]	n.d.[k]	34	34	31	1	0	0	n.d.[k]	n.d.[k]	n.d.[k]	n.d.[k]	n.d.[k]	n.d.[k]
Pt1Cu2	23.8	1.8	3.8	2.2	60	11	18	11	0	0	47	4	7	14	16	12
Pt1Cu6	9.3	3.0	3.3	0.1	60	10	18	12	Trace[h]	0	27	Trace[h]	52	17[l]	4	Trace[h]
Pt1Cu9	10.2	1.4	2.5	1.4	70	0	13	17	0	0	24	Trace[h]	4	31	27	14
Pt1Cu18	12.3	1.4	2.5	1.4	55	0	10	28	7	0	23	1	6	30	26	14

[a] After 5 min on stream.
[b] Turnover frequency, calculated as activity per exposed Pt atom.
[c] After 70 h on stream.
[d] $CHF_2Cl + CH_3F + CHF_3 + CH_2FCl$.
[e] $C_2H_4 + C_2H_6$.
[f] $C_3H_6 + C_3H_8$.
[g] Hydrocarbons C_{4+}.
[h] Traces.
[i] After 5 h on stream.
[j] After the reduction in flowing H_2 the catalyst was treated in a 10% $HCl + N_2$ flow at 523 K for 20 h.
[k] Not determined.
[l] Including 10% C_2F_4.

conversion initially increased for ∼5 h on stream and then the catalysts continuously deactivated (Table 2). After approximately 70 h on stream, the conversion for the Pt/C decreased by 8 times compared to the highest conversion; the conversion for the Pt1Cu6/C catalyzed reaction decreased by 30 times. The final conversions for the Pt1Cu2/C, Pt1Cu9/C, and Pt1Cu18/C were approximately 56% of their highest value.

The Pt/C exhibited negligible selectivity toward CF_2Cl_2 oligomerization products. The selectivity was 1% initially and increased to 5% in 70 h on stream (Table 2), consistent with previous investigations [31,32]. Ethylene was the main C_{2+} product formed on the Pt/C, independent of the TOS. The initial selectivity toward oligomerization products was 11% for the Pt1Cu2/C and increased with increasing Cu/Pt atomic ratio to 35% for the Pt1Cu18/C. The Pt1Cu18/C was the only catalyst that catalyzed the formation of C_3 hydrocarbons at 5 min on stream. The oligomerization products of the other Pt–Cu catalysts at 5 min on stream consisted of only ethylene and ethane.

The oligomerization selectivity of all the bimetallic catalysts increased with TOS. After the 70 h on stream the oligomerization selectivity was 42% for the Pt1Cu2/C and ∼70% for the Pt1Cu9/C and Pt1Cu18/C (Table 2), and significant amount of C_3 and C_{4+} hydrocarbons were formed in addition to the ethylene and ethane. However, the Pt1Cu6/C demonstrated an anomalous TOS performance. Its final oligomerization selectivity was 21%, less than that of Pt1Cu2/C, which contained less Cu (Table 2). Approximately half of the C_{2+} selectivity of the Pt1Cu6/C catalyst was *tetrafluoroethylene*. In addition, unlike the other Pt–Cu catalysts, the oligomerization selectivity of the Pt1Cu6/C passed through a maximum during the course of the $CF_2Cl_2 + H_2$ reaction. After 10 h on stream the reaction products over the Pt1Cu6/C consisted of 55% of the C_{2+} hydrocarbons and 1% of C_2F_4.

The selectivity toward C_1 products also changed with TOS. For the Pt/C, after 5 min on stream the main C_1 products of the $CF_2Cl_2 + H_2$ reaction were CH_4 (15%), CF_2H_2 (53%), CH_3F (15%) and CHF_2Cl (17%) (Table 2). The CH_4 selectivity gradually increased with TOS at the expense of CH_2F_2 to reach 65% in 5 h and then decreased to 40% after 70 h on stream. Exposure of the reduced Pt/C to a 10% HCl + N_2 flow at 523 K for 20 h resulted in the initial CH_4 and CH_2F_2 selectivities of 34% each (Table 2). The distribution of the other C_1 products showed a very weak dependence on TOS and catalyst pretreatment.

The main initial C_1 product of the $CF_2Cl_2 + H_2$ reaction formed with the Pt–Cu catalysts was CH_4 with selectivities in the range of 55–70% (Table 2). Another C_1 product formed initially in significant quantity with the Pt–Cu catalysts was CHF_2Cl. Difluoromethane (CH_2F_2) was observed only with the Pt1Cu2/C and Pt1Cu6/C and the selectivity was <10%. The selectivity toward CH_4 for all Pt–Cu catalysts continuously decreased with TOS. The CH_4 selectivity decreased from 60 to 47% for Pt1Cu2, from 60 to 27% for Pt1Cu6, from 70 to 24% for Pt1Cu9 and from 58 to 23% for Pt1Cu18 after 70 h on stream. The difluoromethane selectivity was about 5% for Pt1Cu2 for the entire length of the experiment. For the other Pt–Cu catalysts only traces of CH_2F_2 were detected. Trifluoromethane was produced only for Pt1Cu6. The selectivity was 20% at 12 h on stream and reached 35% after 70 h. The selectivity trend for CHF_2Cl varied with Cu content. During the kinetics experiments CHF_2Cl selectivity decreased from 16 to 7% for Pt1Cu2/C, from 13 to ∼4% for Pt1Cu9/C, from 10 to 6% for Pt1Cu18/C, but remained unchanged for the Pt1Cu6/C.

4. Discussion

The experimental results described in the previous section raise the following points that require further consideration. (i) According to the TEM results, metallic particles have crystallographic characteristics indistinguishable of those of metallic Pt, regardless of the Cu content. The bimetallic catalysts also contain particles of CuO and isolated or associated Cu ions. (ii) The average particle sizes determined form the TEM images and from the CO chemisorption data are in good agreement for the Pt/C, but they essentially differ for the Pt–Cu catalysts (Table 1). (iii) Despite the fact that monometallic Pt particles do not catalyze the CF_2Cl_2 dehalogenative coupling reaction [31,32] and monometallic Cu catalysts are completely inactive in the $CF_2Cl_2 + H_2$ reaction [32], the coupling selectivity of the Pt–Cu/C catalysts increases with increasing the Cu loading (Table 2). (iv) Even though the average size of metallic particles decreases during the 70 h reaction, all catalysts substantially

deactivate with TOS. A more detailed understanding of the molecular level chemistry associated with these controversies is discussed below.

4.1. Catalyst microstructure

According to the TEM results, all of the Pt in Pt/C catalysts reduces to the metallic state during 1 h reduction at 673 K by flowing H_2 to form particles of preferentially 20–30 Å in size evenly distributed over the support surface (Figs. 1 and 2). Exposure of the catalyst to the $CF_2Cl_2 + H_2$ reaction mixture at 525 K for 70 h decreases the metal particle size from 30 to 17 Å (Fig. 1). This is not surprising given well-known ability of Cl-containing molecules to redisperse supported Pt via the formation/decomposition of labile and mobile Pt chlorides [42–45]. Indirect evidence supporting this mechanism of redispersion comes from the presence of $PtCl_2$ particles in the catalyst exposed to the reaction mixture. Although the formation of Pt fluorides is thermodynamically more favorable than Pt chlorides, the former compounds were not detected in the used Pt/C probably because of their low stability, especially at elevated temperatures [46,47].

Exposure of the reduced Pt/C to a flow of 10% $HCl + N_2$ also led to the redispersion of the supported metallic Pt particles (Table 1). It is quite surprising, because the reaction of Pt and HCl to form $PtCl_2$ (or another Pt chloride) and H_2 is thermodynamically unfavorable [38]. Apparently, because the H_2 evolved in the reaction (4)

$$\mathrm{Pt} + n\mathrm{HCl} \rightarrow \mathrm{PtCl}_n + \tfrac{1}{2}n\mathrm{H}_2 \quad (4)$$

leaves the system with the $HCl + N_2$ flow, the chemical equilibrium shifts to the right. The reaction of HCl with the Pt accounts for both particle redistribution and the formation of non-metallic particles with interlayer distance of 3.6 Å on the support surface. Even though the chemical nature of these particles was not established, it is reasonable to suggest that they are a mixture of Pt chlorides of different stoichiometry.

At a first glance, addition of Cu to the Pt catalyst has only an additive effect. Alloy particles were not detected by HRTEM, and the Pt–Cu/C catalysts consisted of Pt particles of the approximately same sizes as those of Pt/C (Table 1), large particles of CuO and Cu ions. The Cu ions are likely stabilized at cation-exchanged sites such as carboxyl groups or phenolic hydroxyls that are always present on the surface of activated carbons [48]. The presence of Cu oxide is likely because of exposure of the catalysts to air for the preparation of the samples for the TEM investigation. Before exposure to air the oxide particles would have been either that of metallic Cu or particles of $CuCl_2$. Exposure of the Pt–Cu catalysts to the reaction mixture results in a redispersion of Pt particles; but, according to the TEM results, this does not enhance alloying between Pt and Cu. However, the catalytic properties of the Pt–Cu/C are not additive relative to the behavior observed for Pt and Cu (Table 2).

Considering the large surface area of the carbon support and low metal loading (<3%), it is reasonable to suggest, a priori, that the metal precursors will be highly dispersed over the support surface. However, Cu and Pt chlorides in the "as-prepared" Pt–Cu catalysts may be located apart of each other because of chromatographic separation of ions as the impregnating solution passes through the pore structure [49]. If this is the case, the mixing of the metallic components should, therefore, be achieved during catalyst reduction. The degree of mixing will be determined by the relative rates of the Pt and Cu chlorides reduction to the metal and the rates of surface diffusion given the fact that surface diffusion of chlorides is much greater than that of metals [38,42–45]. Thus, if both Pt and Cu chlorides reduce fast to form metallic particles, the degree of alloying will be low. If the rate of chlorides reduction is comparable with the rate of their surface diffusion or is lower, the surface diffusion of the chlorides would compensate for chromatographic separation of Pt and Cu that may take place during the catalyst preparation and the degree of alloying in the reduced catalysts will be higher.

It is well known that Pt chlorides reduce readily with H_2 to the metallic state [38], whereas the reducibility of supported Cu(II) compounds is much lower [50]—probably due to the fact that Cu poorly dissociate H_2 [51]. Thus, for the Pt–Cu catalysts, alloy formation can be described by a "catalyzed reduction" model [52–55], where the Pt particles form first and then mobile Cu(II) ions that diffuse onto these Pt particles swiftly are reduced thereon by surface H atoms [56,57]. The resulting bimetallic particles consist of a Pt core covered with Cu. When the temperature increases, the Cu diffuses into Pt to form a Pt–Cu solid solution. However, even after 2 h reduction at 723 K

with a Pt–Cu/NaY catalyst the surface of the Pt–Cu particles is still enriched in Cu [56]. Our TEM study provides evidence that the situation may be quite different for carbon-supported Pt–Cu catalysts. As the H atoms adsorbed on Pt easily spill over to the carbon support [58], there is a supply of H atoms to reduce $CuCl_2$ particles located apart of Pt to the metallic state thereby limiting the number of migrating $CuCl_2$ molecules. This results in only a small amount of Cu deposited on the surface of the Pt particles that it is undetectable by SAD. This Cu may form Pt–Cu alloy only within the first few atomic layers and would not diffuse into the bulk of Pt particles during catalytic experiments, because the presence of Cl in the reaction mixture causes surface enrichment in Cu due to higher energy of Cl adsorption on Cu than on Pt [59–61].

The suggestion that the surface of Pt particles in the Pt–Cu/C catalysts is partially covered with Cu is also supported by the CO chemisorption data (Table 2). If there were no Cu on the surface of Pt particles, there would be a good agreement for the Pt–Cu/C catalysts between average particle diameters determined by TEM and those calculated from the CO chemisorption data according to formula (1). However, the fact that the TEM numbers are consistently smaller than the chemisorption results suggests that a fraction of Pt particle surface is inaccessible for the CO chemisorption.

4.2. Catalytic performance

As the selectivity of the Pt/C toward the CF_2Cl_2 dechlorinative oligomerization products is very low (5%, Table 2) and the Cu/C is completely inactive in the $CF_2Cl_2 + H_2$ reaction [32], it is tempting to suggest that mixed Pt–Cu sites are responsible for the oligomerization selectivity. Considering the possible reaction mechanism at least two options exist. The first one is that electronic modification of Pt with Cu makes the former metal selective toward CF_2Cl_2 oligomerization. The second option is that Cu is responsible for the oligomerization selectivity, because adjacent Pt atoms promote the Cu activity.

To the best of our knowledge, the data on the electronic state of carbon-supported Pt–Cu catalysts are absent in literature. Perhaps, it is because the IR study of CO adsorption, the most common technique to probe the electronic state of supported metals, is inapplicable to the carbon-supported catalysts due to high ability of the support to absorb the IR irradiation. However, such data are available for the silica-supported Pt–Cu catalysts and, thus, can be used for the interpretation of the catalytic performance of the Pt–Cu/C. It was shown elsewhere [62] that the electronic state of Pt in both an ethylene selective and unselective in the $CH_2Cl–CH_2Cl + H_2$ reaction Pt–Cu/SiO_2 catalysts is similar. However, it differs from the electronic sate of Pt in Pt/SiO_2 that is also an ethylene unselective catalyst. Hence, it was concluded that electronic modification of Pt in Pt–Cu/SiO_2 was unimportant in the hydrogen assisted 1,2-dichloroethane dechlorination to ethylene. As in this reaction both carbon- [63] and silica-supported catalysts [62] behaved similar, there is no reason to suggest that the electronic modification of Pt plays a role in the dehalogenative oligomerization of CF_2Cl_2.

Thus, the second option that Cu is responsible for the oligomerization products appears more plausible. This option is also consistent with the fact that adsorbed CH_x species, the likely intermediate of the CF_2Cl_2 dehalogenative oligomerization, readily couple on Cu surfaces [34], whereas no coupling occurs on Pt, at least, in the presence of coadsorbed halogen atoms [64–66]. The mechanism of promoting the activity of Cu with Pt may be the following. Whereas the dissociative H_2 adsorption is an activated process on Cu [51], H_2 readily dissociates on Pt atoms in the Cu matrix [67]. The H atoms diffuse to the adjacent Cu sites and react thereon with adsorbed halogen atoms to form HCl and HF that desorb to regenerate the active sites. Even though, according to the TEM results, the bulk composition of the Pt-containing particles is independent of the Cu loading in the catalysts, the catalysts with higher the Cu/Pt ratios must have more Cu on the surface of the particles than those with lower Cu/Pt ratios. As the Pt–Cu solid solutions are exothermic [68], an increase in the Cu concentration at the surface of Pt particles will result in splitting Pt ensembles rather than the growth of Cu islands. Thus, the more Cu on the surface, the more Cu atoms have adjacent Pt atoms which will dissociate H_2 to clean the Cu of adsorbed halogen atoms during CF_2Cl_2 dehalogenative oligomerization. Moreover, the dilution of Pt with Cu may result in a suppression of hydrogenation chemistry on Pt. If a CF_2Cl_2 molecule dissociate on a site consisting, say, one Pt and six Cu atoms (a fragment of the $Cu_3Pt(1\,1\,1)$ surface), it is reasonable to

expect that this site would couple the reaction intermediate rather than hydrogenate it to form CH_4. All this is consistent with the experimental observation in terms of the coupling selectivity of the Pt–Cu/C catalysts (Table 2).

The fact that the formation of significant amount of fluorinated coupling products was not observed for the Pt–Cu/C catalysts with the exception of Pt1Cu6/C after long TOS suggests that formation of the oligomerization product occurs via a mechanism similar to the "carbide" mechanism of the Fischer–Tropsch reaction [69]. The first step of the reaction is the dissociation of all metal halogen bonds of the CF_2Cl_2 molecules to form carbon. The carbon atoms would hydrogenate to CH_x species that couple on the surface and form the C_{2+} hydrocarbons. It is unlikely that an association of bare carbon atoms followed by their hydrogenation results in the oligomerization products because such process leads to the formation of carbonaceous deposits that are much less reactive toward H atoms than the bare C atoms. In general, the CH, CH_2 and CH_3 species can be the reaction intermediate of coupling. However, the coupling of two methyl groups on the surface to form ethane is highly unlikely because of sterical hindrance [70]. According to the theoretical considerations, this reaction would have very high activation barrier [71]. The coupling of the CH species does not look likely either because acetylene was not detected among the oligomerization products over the Pt–Cu/C catalysts. Thus, the surface carbene, CH_2, is a likely precursor of the oligomerization products. The barrier for CH_2 migration over metal surfaces is low, the coupling of two methylenes is exothermic and no energy barrier exists along the reaction path [71]. However, the possibility of the coupling reaction between CH and CH_2 species to form surface vinyl, $CH{=}CH_2$, cannot be ruled out. This pathway was recently suggested for the hydrocarbon chain growth in the Fischer–Tropsch reaction [72].

The formation of carbon on the surface of the Pt–Cu catalysts as a first step of the dehalogenation reaction may be closely associated with catalyst deactivation. If the rate of carbon hydrogenation is lower than that of carbon polymerization to form carbonaceous deposits, the catalyst will deactivate. The very well-known ability of Pt to decompose hydrocarbons adsorbed on its surface and reluctance of Cu to dissociate C–H bonds [34] suggest that the equilibrium constant of the reaction (5) on Cu is larger than

$$C_{(surf.)} + xH_{(surf.)} \leftrightarrow CH_{x(surf.)} \quad (5)$$

that on Pt. It means that catalyst deactivation would be predominantly caused by carbon deposition on Pt. The deactivation of the bimetallic catalysts is accompanied with a decrease in the selectivity toward CH_4 and the C_1 products of CF_2Cl_2 partial dehalogenation that is consistent with the suggestion that all C_1 reaction products form on the Pt sites.

5. Conclusion

Activated carbon-supported Pt–Cu catalysts with a Cu to Pt atomic ratio in the range of 2–18 catalyze the formation of oligomerization hydrocarbon products from an equimolar mixture CF_2Cl_2 and H_2 at 523 K. The oligomerization selectivity is a function of Cu/Pt atomic ratio. This selectivity is low initially when mainly CH_4 and partially dehalogenated C_1 products form. However, the C_{2+} product selectivity increases with TOS to exceed 70% for the catalysts with Cu/Pt ratio greater than 6. The combination of high resolution transmission microscopy and CO chemisorption measurements provide evidence that the active moieties of the Pt–Cu/C catalysts are the Pt–Cu particles with Cu being segregated to the surface. The average sizes of the particles decrease resulting from the exposure of the reduced catalysts to the reaction mixture. Thus, the observed catalyst deactivation is related rather to carbon deposition during $CF_2Cl_2 + H_2$ reaction than to sintering. The performance of the catalysts in the $CF_2Cl_2 + H_2$ reaction is consistent with the hypothesis that the formation of oligomerization products occurs on Cu sites, whereas Pt is responsible for the formation of CH_4 and the C_1 products of the partial CF_2Cl_2 dehalogenation. Additionally, Pt provides supply of dissociated H atoms that diffuse to the Cu sites cleaning them of the adsorbed halogen atoms.

Acknowledgements

Support from the National Science Foundation (CTS 0086638) is gratefully acknowledged.

References

[1] W. Brune, Nature 379 (1996) 486–487.
[2] Alternative Fluorocarbons Environmental Acceptability Study. http://www.afeas.org/production_and_sales.html.
[3] Y.H. Choi, W.Y. Lee, J. Mol. Catal. A 174 (2001) 193–204.
[4] B. Coq, J.M. Cognion, F. Figuéras, D. Tornigant, J. Catal. 141 (1993) 21–33.
[5] B. Coq, S. Hub, F. Figuéras, D. Tornigant, Appl. Catal. A 101 (1993) 41–51.
[6] B. Coq, F. Figuéras, S. Hub, D. Tornigant, J. Phys. Chem. 99 (1995) 11159–11166.
[7] A. Morato, C. Alonso, F. Medina, Y. Cesteros, P. Salagre, J.E. Sueiras, D. Tichit, B. Coq, Appl. Catal. B 32 (2001) 167–179.
[8] A. Wiersma, E.J.A.X. van de Sandt, M. Makkee, H. van Bekkum, J.A. Moulijn, Stud. Surf. Sci. Catal. 101 (1996) 369–378.
[9] A. Wiersma, E.J.A.X. van de Sandt, M. Makkee, C.P. Luteijn, H. van Bekkum, J.A. Moulijn, Catal. Today 27 (1996) 257–264.
[10] A. Wiersma, E.J.A.X. van de Sandt, H. van Bekkum, J.A. Moulijn, Appl. Catal. A 155 (1997) 59–73.
[11] E.J.A.X. van de Sandt, A. Wiersma, M.A. den Hollander, H. van Bekkum, M. Makkee, J.A. Moulijn, J. Catal. 177 (1998) 29–39.
[12] S.S. Deshmukh, J.L. d'Itri, Catal. Today 40 (1998) 377–385.
[13] K.O. Early, V.I. Kovalchuk, F. Lonyi, S.S. Deshmukh, J.L. d'Itri, J. Catal. 182 (1999) 219–227.
[14] W. Juszczyk, A. Malinowski, Z. Karpiński, Appl. Catal. A 166 (1998) 311–319.
[15] A. Malinowski, W. Juszczyk, M. Bonarowska, J. Pielaszek, Z. Karpiński, J. Catal. 177 (1998) 153–163.
[16] A. Malinowski, W. Juszczyk, J. Pielaszek, M. Bonarowska, M. Wojciechowska, Z. Karpiński, Chem. Commun. (1999) 685–686.
[17] M. Bonarowska, B. Burda, W. Juszczyk, J. Pielaszek, Z. Kowalczyk, Z. Karpiński, Appl. Catal. B 35 (2001) 13–20.
[18] M. Bonarowska, A. Malinowski, W. Juszczyk, Z. Karpiński, Appl. Catal. B 30 (2001) 187–193.
[19] M. Bonarowska, J. Pielaszek, V.A. Semikolenov, Z. Karpiński, J. Catal. 209 (2002) 528–538.
[20] B.S. Ahn, S.C. Lee, D.J. Moon, B.G. Lee, J. Mol. Catal. A 106 (1996) 83–91.
[21] B.S. Ahn, S.G. Jeon, H. Lee, K.Y. Park, Y.G. Shul, Appl. Catal. A 193 (2000) 87–93.
[22] M. Ökal, M. Maciejewski, A. Baiker, Appl. Catal. B 21 (1999) 279–289.
[23] A.L.D. Ramos, M. Schmal, D.A.G. Aranda, G.A. Somorjai, J. Catal. 192 (2000) 423–431.
[24] Y.C. Cao, X.Z. Jiang, W.H. Song, Z.Q. Bai, X.Q. Fang, Catal. Lett. 76 (2001) 53–57.
[25] Y.C. Cao, X.Z. Jiang, J. Mol. Catal. A 184 (2002) 183–189.
[26] M.J. Krishna, S.S. Chandra, V.S. Kumar, R.K.S. Rama, Catal. Commun. 3 (2002) 149–149.
[27] Y.C. Cao, X.Z. Jiang, Ind. J. Chem. A 41 (2002) 1607–1611.
[28] S.S. Chandra, M.J. Krishna, R.P. Kanta, R.K.S. Rama, Catal. Commun. 4 (2003) 39–44.
[29] E.J.A.X. van de Sandt, A. Wiersma, M. Makkee, H. van Bekkum, J.A. Moulijn, Appl. Catal. A 155 (1997) 59–73.
[30] A. Morato, C. Alonso, F. Medina, P. Salagre, J.P. Sueiras, R. Terrado, A. Giralt, Appl. Catal. B 23 (1999) 175–185.
[31] P.P. Kulkarni, S.S. Deshmukh, V.I. Kovalchuk, J.L. d'Itri, Catal. Lett. 61 (1999) 161–166.
[32] P.P. Kulkarni, V.I. Kovalchuk, J.L. d'Itri, Appl. Catal. B 36 (2002) 299–309.
[33] B. Coq, F. Figuéras, J. Mol. Catal. A 173 (2001) 117–134.
[34] M.X. Yang, S. Sarkar, B.E. Bent, S.R. Bare, M.T. Holbrook, Langmuir 13 (1997) 229–242.
[35] T.B. Massalski, H. Okamoto, P.R. Subramanian, L. Kacprzak (Eds.), Binary Alloys Phase Diagrams, vol. 2, ASM International, 1990, pp. 1460–1462.
[36] M.I. Bruce, J. Organomet. Chem. 44 (1972) 209–226.
[37] P. Hollins, Surf. Sci. Rep. 16 (1992) 51–94.
[38] J.R. Anderson, Structure of Metallic Catalysts, Academic Press, London, 1975.
[39] DataBase PDF-2, JCPDS Nos. 16-0064, 40-1287, 1997.
[40] DataBase PDF-2, JCPDS No. 45-0937, 1997.
[41] J.M. Cowley, Diffraction Physics, Elsevier, Amsterdam, 1995.
[42] P. Birke, S. Engels, K. Becker, H.-D. Neubauer, CHEMTECH 31 (1979) 473–479.
[43] C.S. Kellner, J.J. Lerou, V. Rao, K.G. Wuttke, World Patent Appl. WO 91/04097 (1991).
[44] K. Foger, H. Jaeger, J. Catal. 92 (1985) 64–78.
[45] M.J. D'Aniello, D.R. Monroe, C.J. Carr, M.H. Krueger, J. Catal. 109 (1988) 407–422.
[46] F.A. Cotton, G. Wilkinson, Advanced Inorganic Chemistry, Wiley/Interscience, New York, 1988.
[47] S.E. Livingstone, The Chemistry of Ruthenium, Rhodium, Palladium, Osmium, Iridium and Platinum, Pergamon Press, London, 1973.
[48] A.J. Bird, in: A.B. Stiles (Ed.), Catalyst Supports and Supported Catalysts: Theoretical and Applied Concepts, Butterworths, Boston, 1987, pp. 107–137.
[49] V. Ponec, G.C. Bond, Catalysis by Metals and Alloys, Elsevier, Amsterdam, 1995 (Chapter 7).
[50] A. Dandecar, M.A. Vannice, J. Catal. 178 (1998) 621–639.
[51] J.M. Campbell, C.T. Campbell, Surf. Sci. 259 (1991) 1–17.
[52] S.M. Augustine, W.M.H. Sachtler, J. Catal. 106 (1987) 417–427.
[53] S.M. Augustine, W.M.H. Sachtler, J. Phys. Chem. 91 (1987) 5953–5956.
[54] S.M. Augustine, M.S. Nacheff, C.M. Tsang, J.B. Butt, W.M.H. Sachtler, Stud. Surf. Sci. Catal. 38 (1988) 1–10.
[55] S.M. Augustine, M.S. Nacheff, C.M. Tsang, J.B. Butt, W.M.H. Sachtler, in: M.J. Phillips, M. Ternan (Eds.), Proceedings of the Ninth International Congress on Catalysts, Calgary, April 1988, Chemical Institute of Canada, Ottawa, l988, pp. 1190–1197.
[56] G. Moretti, W.M.H. Sachtler, J. Catal. 115 (1989) 205–216.
[57] D.H. Ahn, J.S. Lee, M. Nomura, W.M.H. Sachtler, G. Moretti, S.I. Woo, R. Ryoo, J. Catal. 133 (1992) 191–201.
[58] A.J. Robell, E.V. Ballou, M. Boudart, J. Phys. Chem. 68 (1964) 2748–2753.
[59] P.J. Goddart, R.M. Lambert, Surf. Sci. 67 (1977) 180–194.

[60] W. Erley, Surf. Sci. 94 (1980) 281–292.
[61] W. Erley, Surf. Sci. 114 (1982) 47–64.
[62] L.S. Vadlamannati, D.R. Luebke, V.I. Kovalchuk, J.L. d'Itri, Stud. Surf. Sci. Catal. 130 (2000) 233–238.
[63] L.S. Vadlamannati, V.I. Kovalchuk, J.L. d'Itri, Catal. Lett. 58 (1999) 173–178.
[64] F. Zaera, Langmuir 7 (1991) 1998–1999.
[65] F. Zaera, R. Hoffman, J. Phys. Chem. 95 (1991) 6297–6303.
[66] F. Solymosi, Catal. Today 28 (1996) 193–203.
[67] R. Linke, U. Schneider, H. Busse, C. Becker, U. Schröder, G.R. Castro, K. Wandelt, Surf. Sci. 307–309 (1994) 407–411.
[68] R. Hultgren, P.D. Desai, D.T. Hawkins, M. Gleiser, K.K. Kelley, Selected Values of the Thermodynamic Properties of Binary Alloys, American Society for Metals, Metals Park, OH, 1973.
[69] H.H. Storch, N. Golumbic, R.B. Anderson, The Fischer–Tropsch and Related Syntheses, Wiley, New York, 1951.
[70] A. Paul, B.E. Bent, J. Catal. 147 (1994) 264–271.
[71] C. Zheng, Y. Apeloig, R. Hoffman, J. Am. Chem. Soc. 110 (1988) 749–774.
[72] P.M. Maitlis, R. Quyoum, H.C. Long, M.L. Turner, Appl. Catal. A 186 (1999) 363–374.